A Lead-Lag Filter for Virtual Synchronous Machines with Improved Electromechanical Damping

A Lead-Lag Filter for Virtual Synchronous Machines with Improved Electromechanical Damping

Fabio Mandrile, Vincenzo Mallemaci, Enrico Carpaneto and Radu Bojoi
Dipartimento Energia "G.Ferraris"
Politecnico di Torino
Torino, Italy
fabio.mandrile@polito.it

***Abstract*—Traditional power systems based on synchronous generators often feature low frequency electromechanical oscillations. However, the integration of renewable energy sources through power converters can help tackling this issue. In fact, thanks to the concept of Virtual Synchronous Machine (VSM), it is possible to make the inverters behave as real synchronous machines (SMs). This way, the inverters can be integrated into the grid as traditional SMs and can even outperform them when it comes to damping low frequency oscillations in the power system. In order to do that, proper damping algorithms must be adopted in the VSM model. Therefore, this paper presents a simple and straighforward damping method for VSMs based on a single lead-lag filter acting on the VSM active power feedback.The proposed method and its integration in the VSM model are described. Then, the proposed solution has been experimentally compared to conventional methods, along with comparison metrics, to highlight its benefits.**

***Index Terms*—Virtual Synchronous Machine (VSM), Electromechanical Damping, Lead-lag filter, Renewable Energy Sources**

I. Introduction

Modern power systems are facing the challenge of integrating renewable energy sources (RESs) into the electric grid. Differently from traditional synchronous sources (e.g., thermal plants), many RESs are interfaced to the grid through power converters. Most control methods available for these sources are based on maximum power point tracking (MPPT) algorithms, with the goal of always injecting the maximum power available on the source side. However, this MPPT logic relies on the still prevalent presence of synchronous machines (SMs) in the grid and it may lead to frequency stability issues under large penetration of RESs. To tackle this issue, it is possible to make static converters more grid friendly, using proper control algorithms, such as the concept of virtual synchronous machine (VSM) [1]–[3]. This way, electronic converters are enabled to provide key ancillary services to the grid, such as virtual inertia and reactive support during grid faults. Moreover, VSMs have some key advantages compared to real SMs. First, VSMs do not have physical electromagnetic limitations of the real SMs (e.g., saturation, couplings, etc...) and their parameters can be adapted to the instantaneous grid conditions, being digital control algorithms. Second, the dynamic behavior of VSMs is much faster than SMs, as it only depends on the digital control bandwidth (hundreds of Hz or kHz) and it is not limited by the thermal and mechanical transients of traditional plants (e.g., thermal power plants).

Therefore, while SMs are affected by a limited electromechanical damping and cannot easily counteract low frequency power oscillations (range few Hz) due to the limited dynamics of their prime movers (e.g., thermal plants), VSMs are capable of tackling these issues and improving the performance of the power system in terms of oscillations damping.

However, in order to accomplish this goal, it is necessary to implement an effective damping algorithm in the VSM model. To this purpose, several strategies have been reported in the technical literature [4]:

- Damping implemented in the emulated swing equation [5] of the VSM, proportional to the difference between the VSM speed and the nominal grid frequency [6] (droop-damping);
- Damping proportional to the speed difference between the VSM and the actual grid frequency measured by a phase locked loop (PLL) [7] (PLL-damping);
- Damping power proportional to the VSM virtual acceleration [8];
- Virtual dampers and modified virtual impendances [9]–[11].

While all these methods guarantee the necessary damping to VSMs, they often suffer of several drawbacks, such as the coupling between the damping and the active droop action [11], the need of an additional phase locked loop (PLL) [7], numerical derivatives [4] or additional non necessary complexity added to the model, such as the modification of the virtual stator circuit [10].

To solve these drawbacks, this paper proposes a simple damping method for VSMs based on a single lead-lag filter on its virtual power feedback. The proposed solution does not couple the damping and the active droop action (unlike droop-damping), does not require additional control parts (unlike PLL-damping) and does not require complex tuning or extra computational burden to the model. The proposed method is here applied to a VSM implementation available in the

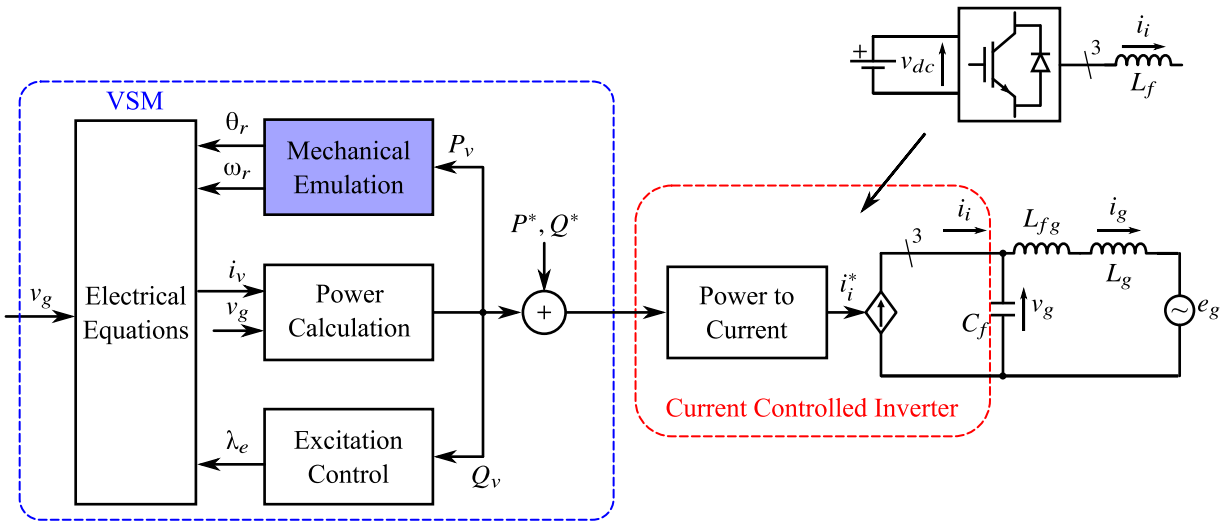

Fig. 1: Block diagram of the considered VSM controlling a grid-feeding inverter. The proposed lead-lag damping is implemented inside the mechanical emulation block (highlighted in blue).

literature [12], but it can be easily extended to other models, being a filter on the feedback active power.

The proposed damping method is described in Section II. Then, in Section III the tuning process of the proposed solution is described step-by-step. The conventional damping techniques against which the proposed one is compared are described in Section IV. Finally, in Section V the proposed solution is validated experimentally and compared to the conventional ones.

II. Lead-Lag Damping Description

The considered system is a VSM-driven current controlled inverter connected to the grid, as described in the block diagram of Fig. 1. The VSM generates the active and reactive power references P_v, Q_v to the inverter current controller [12]. The VSM is composed of the following functional blocks:

1) **Mechanical emulation** – this block emulates the mechanical behavior of the VSM, regulating the transfer of active power. This block generates both the active power reference P_v and the orientation of the current controller;
2) **Electrical equation** – this block implements the virtual stator of the VSM, receiving the measured grid voltage v_g, the VSM speed ω_r and the virtual excitation flux linkage λ_e;
3) **Excitation control** – this regulates the exchange of reactive power [13];
4) **Power calculation** – calculates the virtual power of the VSM by multiplying its current i_v and the grid voltage v_g.

The proposed damping strategy only modifies the mechanical emulation block of the VSM. As shown in Fig. 2, the mechanical emulation is performed by implementing the well-known swing equation of SMs [5]. The term of the swing equation modeling the equivalent damping of the machine,

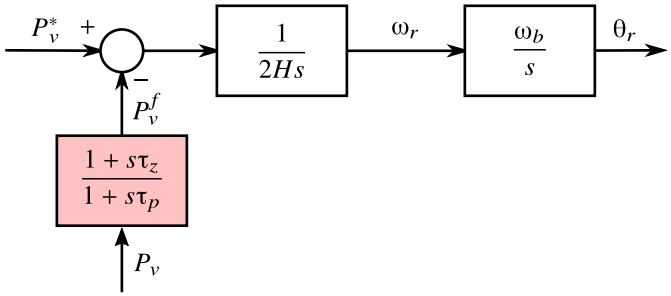

Fig. 2: Diagram of the mechanical emulation block with the proposed lead-lag damping (highlighted in red).

proportional to the difference between the virtual speed ω_r and the rated grid speed ω_n is however excluded, as the damping is provided by the proposed lead-lag technique. Therefore, the mechanical emulation is simplified (see Fig. 2) and it is divided into two stages:

1) Inertial part of the rotor, calculating the virtual rotor speed ω_r from the power error $P_v^* - P_v^f$, depending on the inertia constant H;
2) The rotor angle θ_r calculation from the virtual rotor speed ω_r (since the model is here expressed in per unit, it is necessary to define the base angular speed ω_b).

The proposed damping method modifies the mechanical emulation by adding a lead-lag filter on the feedback active power P_v of the VSM. The filtered active power P_v^f is then fed to the rest of the mechanical emulation block, as depicted in Fig. 2. The proposed damping method is based on a lead-lag filter defined as

$$LL(s) = \frac{1 + s\tau_z}{1 + s\tau_p} \tag{1}$$

where the time constants of the pole τ_p and of the zero τ_z are the only two required parameters.

III. Parameter Tuning

The two parameters of the proposed lead-lag filter τ_z and τ_p must be tuned in order to ensure the proper damping to the virtual machine. The two parameters τ_p and τ_z of the lead-lag filter are tuned based on the equivalent linearized model of the electromechanical part of the VSM, shown in Fig. 3. In this linearized model the interaction with the grid is modeled according to the traditional power system theory [5]. In particular, the following assumptions [14] are made:

1) The dynamic behavior of the inner current control loop is several orders of magnitude faster than the electromechanical part of the VSM. Therefore, it is simplified with a unity gain transfer function;
2) The virtual stator resistance is neglected, as it is much smaller than the stator and grid reactances in medium and high voltage grids;
3) The virtual flux linkages of the VSM are considered constant in the first instant of the electromechanical transient [5];
4) The VSM is operating at no load, i.e., zero current, and nominal speed ($\omega_r = 1$ pu).

The active power exchange with the grid is therefore $\Delta P_v = k_s \Delta\delta$, where δ is the load angle of the VSM and k_s is the synchronizing power (maximum theoretical active power that can be exchanged with the grid). This power is defined as:

$$k_s = \frac{V_0 E_0}{X_s + X_g} \tag{2}$$

where X_s and X_g are the VSM and grid reactance, respectively, and V_0, E_0 are the grid voltage and the VSM back emf at the linearization point.

The characteristic equation of the linearized system of Fig.3 can be derived as follows:

$$1 + \frac{1}{2Hs}\frac{\omega_b}{s} k_s \frac{1 + s\tau_z}{1 + s\tau_p} = 0 \tag{3}$$

Then, (3) can be rearranged to obtain the following:

$$s^3 + \frac{1}{\tau_p} s^2 + \frac{\omega_b k_s}{2H}\frac{\tau_z}{\tau_p} s + \frac{\omega_b k_s}{2H}\frac{1}{\tau_p} = 0 \tag{4}$$

and the variable a can be defined to simplify the notation:

$$a = \frac{\omega_b k_s}{2H} \tag{5}$$

To better analyze this linearized system, it is useful to compare (4) with a generic third order characteristic equation in the form:

$$(s^2 + 2\zeta\omega_0 s + \omega_0^2)(s + p_r) = 0 \tag{6}$$

This characteristic equation (6) features two complex poles defined by their damping ζ and natural frequency ω_0 and one real pole $-p_r$.

From (4), it emerges that the lead-lag filter parameters are tuned according to the desired electromechanical behavior of the VSM. The needed parameters, which must be provided by the user are the VSM inertia constant H, the synchronizing power k_s (i.e., information on the point of connection) and the desired damping coefficient ζ.

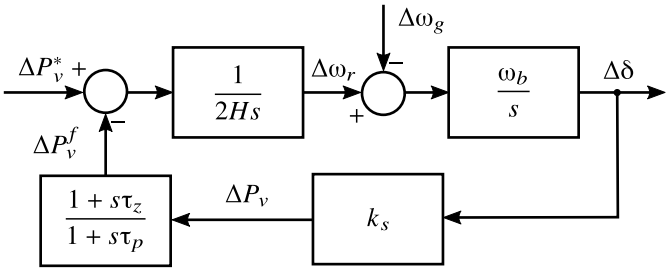

Fig. 3: Linearized model of the electromechanical part of the VSM using the proposed lead-lag damping.

By comparing (4) and (6), the following relationships are found:

$$\begin{aligned} 2\zeta\omega_0 + p_r &= \frac{1}{\tau_p} \\ 2\zeta\omega_0 p_r + \omega_0^2 &= ak \\ \frac{a}{\tau_p} &= \omega_0^2 p_r \end{aligned} \tag{7}$$

where $k = \tau_z/\tau_p$.

Having 4 variables (ω_0, p_r, k, τ_p) and only the three available relationships of (7), it is necessary to introduce an additional equation to uniquely derive the tuning parameters. A possible solution is to minimize the ratio $k = \tau_z/\tau_p$, which means reducing the high frequency gain of the lead-lag filter. This solution guarantees the least sensitivity from high frequency disturbances affecting the grid. Given that the damping coefficient ζ is a design input, it is possible to add the following condition:

$$\frac{\partial k}{\partial \omega_0} = 0 \tag{8}$$

where the minimization depends only on ω_0.

From (7), it is possible to obtain p_r:

$$\begin{aligned} 2\zeta\omega_0 p_r + \omega_0 &= \omega_0 p_r \tau_p \\ p_r &= \frac{\omega_0}{\omega_0\tau_p - 2\zeta} \end{aligned} \tag{9}$$

Then, by substituting (9) into (7):

$$\begin{aligned} 2\zeta\omega_0 + \frac{\omega_0}{\omega_0\tau_p - 2\zeta} &= \frac{1}{\tau_p} \\ 2\zeta\omega_0\tau_z + \frac{\omega_0\tau_z}{\omega_0\tau_p - 2\zeta} &= \frac{\tau_z}{\tau_p} = k \end{aligned} \tag{10}$$

The aforementioned minimization can be now applied to (10) as follows:

$$\begin{aligned}
\frac{\partial k}{\partial \omega_0} &= 0 \\
2\zeta\tau_z + \frac{\tau_z\left(\omega_0\tau_p - 2\zeta\right) - \omega_0\tau_z\tau_p}{\left(\omega_0\tau_p - 2\zeta\right)^2} &= 0 \\
1 - \frac{1}{\left(\omega_0\tau_p - 2\zeta\right)^2} &= 0 \\
\left(\omega_0\tau_p - 2\zeta\right)^2 &= 1 \\
\omega_0\tau_p &= 2\zeta \pm 1
\end{aligned} \tag{11}$$

There are, therefore, two solutions for $\omega_0\tau_p$, which can be used to derive p_r from (9):

$$\begin{aligned}
\omega_0\tau_p &= 2\zeta + 1 \quad \Rightarrow \quad p_r = \omega_0 \\
\omega_0\tau_p &= 2\zeta - 1 \quad \Rightarrow \quad p_r = -\omega_0
\end{aligned} \tag{12}$$

It is evident that the second solution ($\omega_0\tau_p = 2\zeta - 1$) is not acceptable, since it would lead to a real pole in the right half plane for damping coefficient smaller than 1. It is therefore obtained that:

$$\begin{aligned}
\omega_0^2 &= (2\zeta + 1)\, a \\
p_r &= \omega_0 \\
k &= (2\zeta + 1)^2
\end{aligned} \tag{13}$$

The final tuning values of the proposed lead-lag filter are as follows:

$$\begin{aligned}
\tau_p &= \sqrt{\frac{2H}{\omega_b k_s \left(2\zeta + 1\right)^3}} \\
\tau_z &= \sqrt{\frac{2H}{\omega_b k_s}\left(2\zeta + 1\right)}
\end{aligned} \tag{14}$$

IV. Conventional Damping Methods

The proposed solution is compared with the following conventional methods available in the technical literature:

1) **Droop-damping**: damping action proportional to the virtual speed error from nominal value;
2) **PLL-damping**: damping power proportional to the speed error from measured grid frequency;
3) **PI-damping**: a Proportional-Integral (PI) regulator is used in place of the machine virtual rotor.

A. Droop-based Damping

The simplest solution available to provide electromechanical damping to a VSM is the droop-based damping and it is adopted by several models in the literature, such as [6], [15], [16]. This method implements the well known swing equation of synchronous generators [5]:

$$P_m - P_e = 2H\frac{d(\omega_r - \omega_g)}{dt} + D_p(\omega_r - \omega_g) \tag{15}$$

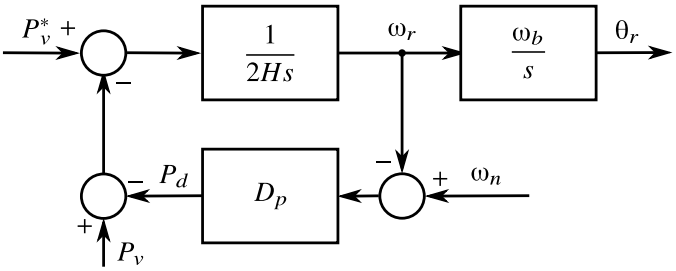

Fig. 4: Diagram of the mechanical emulation block with the droop-based damping.

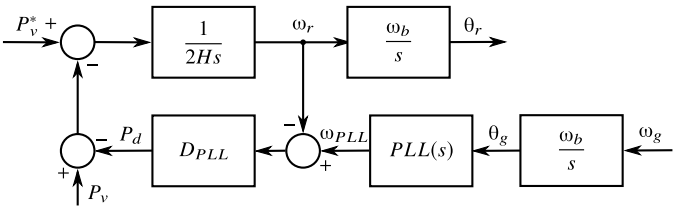

Fig. 5: Diagram of the mechanical emulation block with the PLL-based damping.

imposing the grid frequency ω_g to its nominal value ω_n. This means that the virtual speed ω_r and virtual rotor angle θ_r are calculated from the reference power P^* and the virtual feedback power P_v as follows:

$$\begin{aligned}
2H\frac{d\omega_r}{dt} &= P_v^* - P_v - D_p(\omega_r - \omega_n) \\
\frac{d(\theta_r)}{dt} &= \omega_r
\end{aligned} \tag{16}$$

The resulting block diagram is depicted in Fig. 4.

The tuning of this damping method is performed in a similar way as Section III, leading to a value of the damping coefficient D_p:

$$D_p = \zeta\sqrt{8H\omega_b k_s} \tag{17}$$

B. PLL-based Damping

A second common solution [1], [7], [16] is to use the grid frequency measured by a PLL instead of its nominal value. The implementation of this method is similar to the already presented droop-based damping. Here, (15) is modified and the measured grid frequency ω_{PLL} is used instead of its nominal value ω_n, as shown in Fig. 5.

The tuning procedure is equivalent to the already presented (17) for the droop-based damping. A correction coefficient is however necessary. This correction factor, depending on the machine and grid inductances, is obtained from empirical considerations and from the existing literature [7], [10] as follows:

$$D_{PLL} = D_p\frac{X_s + X_g}{X_s} = \zeta\sqrt{8H\omega_b k_s}\frac{X_s + X_g}{X_s} \tag{18}$$

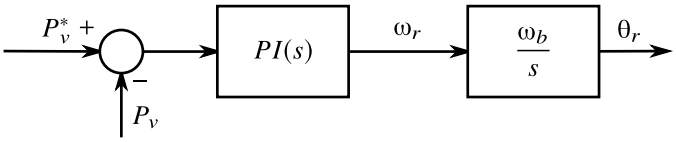

Fig. 6: Diagram of the mechanical emulation block with the PI-based damping.

C. PI-based Damping

The PI-based damping employs a PI regulator to eliminate the steady-state active power error of the VSM [15]. Therefore, the inertial block of the swing equation $(1/2Hs)$ is replaced by a PI regulator (see Fig. 6) defined as:

$$PI(s) = k_d + \frac{k_h}{s} \tag{19}$$

where k_d is the proportional term, providing damping, and k_h is the integral one, in charge of the inertial action.

The two parameters of the PI regulator k_d and k_h must be tuned in order to ensure the proper damping and inertia to the virtual machine. The tuning procedure is similar to the one of the droop-based and PLL-based and it leads to the following tuning values:

$$\begin{aligned} k_d &= 2\zeta\sqrt{\frac{k_h}{k_s\omega_b}} \\ k_h &= \frac{1}{2H} \end{aligned} \tag{20}$$

V. Experimental Validation

A 15 kVA two-level three-phase inverter, controlled at 10 kHz by a dSpace 1005 platform, has been used for experimental validation. The experimental setup is diagrammed in Fig. 7 and depicted in Fig. 8. This inverter is connected to a grid emulator (rated 50 kVA and emulating a 120 Vrms phase voltage grid at 50 Hz) through an LCL filter (L_f = 545 µH, C_f = 22 µF and L_{fg} = 120 µH). An equivalent grid impedance of L_g = 300 µH is placed between the inverter and the grid emulator.

The proposed method has been validated against three conventional methods available in the literature and described in Section IV: Droop-damping, PLL-damping and PI-damping. To ensure a fair comparison, the tuning of all methods was performed using the same inputs (H = 4 s, ζ = 0.7 and k_s = 5 pu).

Two tests were carried out:

1) Grid frequency drop after a major power imbalance. This test checks the coupling between the damping action and the active droop action. If the response is decoupled, no active power is injected after the frequency transient;
2) Voltage dip with phase displacement (−2% voltage and −2° phase jump). This tests the quality of the virtual speed in case of grid disturbances. The smaller the speed variation, the better the rejection. Only a voltage dip was tested, but the same applies for swells, as the model reacts to small signal variations in a symmetrical way.

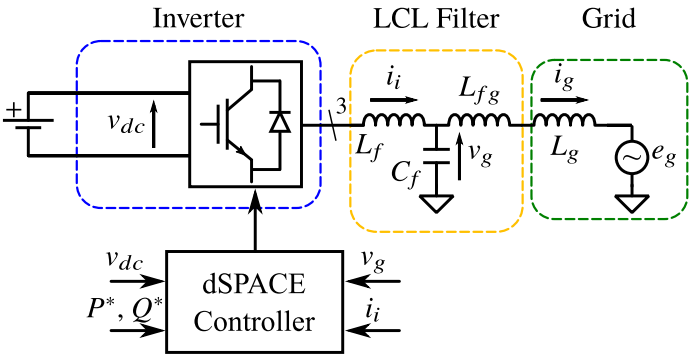

Fig. 7: Block diagram of the experimental setup.

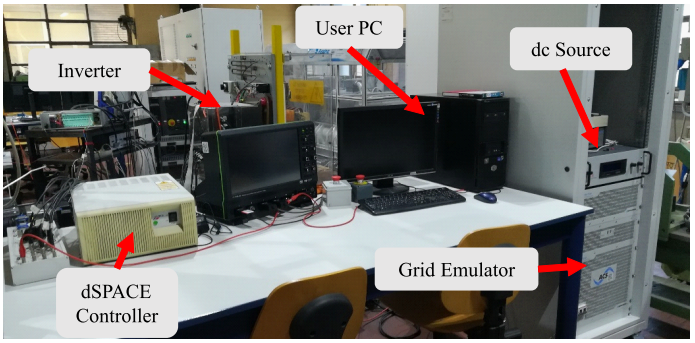

Fig. 8: Picture of the experimental setup.

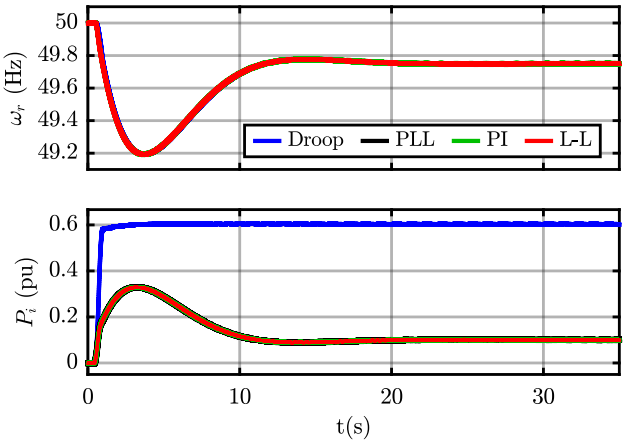

Fig. 9: Test 1. Grid active power imbalance. The response of the proposed lead-lag damping (L-L) against three conventional methods is presented in terms of virtual speed ω_r and active power injection P_i into the grid.

A. Test 1: Grid Frequency Drop

In Test 1 (see Fig. 9) a major power imbalance in the grid is emulated. The grid frequency drops to a nadir of 49.2 Hz and then settles to a final value of 49.75 Hz. The magnitude of the emulated imbalance has been amplified with respect to actual grid fluctuations to highlight the differences between the damping methods. For a fair comparison, an external frequency droop controller (droop gain 5% [5]) was implemented. Each compared method tracks the grid frequency with no oscillations. However, the droop-damping almost immediately saturates the active power injection to the inverter current limit set to 0.6 pu. This unwanted too large power injection is due to the necessary damping gain of the droop-damping (around 10 times larger than standard droop coefficients). The other three methods (PLL-based, PI-based and proposed L-L) feature an inertial behavior in the early phase of the transient and later a proportional regulation of the frequency with a power injection compliant with the designed droop controller. They inject inertial power and active droop power during all the transient. However, in this case, the droop power injection is limited and complies with the design droop coefficient (i.e, an active power when the frequency stabilizes equal to 0.1 pu). In conclusion, the droop-based damping is much inferior compared to the other damping methods, as it injects a too large active power when the grid frequency is far from its rated value. The other damping methods are equivalent under this aspect.

B. Test 2: Voltage Dip

In Test 2 (see Fig. 10), the VSM was perturbed by an emulated -2% voltage dip with a -2° phase jump. The magnitude of the perturbation was chosen in order to avoid the current limitation of the converter during this test. Since this test verifies the limited sensitivity of the proposed damping method against disturbances, the virtual speed ω_r of the VSM was compared for each considered damping method. In this matter, the droop-damping is superior, since it shows the least sensitivity of the virtual speed to grid disturbances. The other three methods (PLL-based, PI-based and LL-based) are more sensitive to grid disturbances, leading to larger virtual speed deviations. In particular, the PI-based shows the largest speed variation (-150 mHz) and the largest steady-state high frequency oscillations, caused by the current and voltage measurement non ideality. This large variation in the first instants of the perturbation is due to the direct feed-through (related to the proportional term k_d) from the active power feedback to the virtual speed ω_r. Better results, with lower sensitivity, are obtained with the PLL-based and LL-based damping. In this case, the proposed LL-damping is not the best, but represents a good compromise between the solutions, featuring a reduced speed deviation during the perturbation.

C. Summary of Damping Methods

A summary of the presented damping strategies is available in Table I to highlight the key differences of the analyzed methods. The comparison is carried out in terms of number of parameters needed by the damping method, easiness of implementation and the two benchmark experimental tests. From this summary comparison is clear that the proposed lead-lag technique represents a viable solution for the VSMs electromechanical damping, compared to conventional ones.

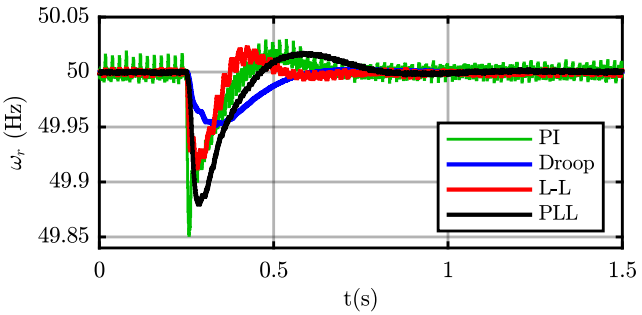

Fig. 10: Test 2. Voltage dip. The virtual speed sensitivity to grid disturbances is validated with a -2% voltage dip and -2° phase jump. The response of the conventional and proposed L-L damping techniques are compared in terms of virtual speed ω_r variations.

TABLE I: SUMMARY OF THE COMPARED DAMPING METHODS FOR VSMS.

Feature	**Droop**	**PLL**	**PI**	**L-L**
Parameters	D_p	D_{PLL}	k_p^{PI},k_i^{PI}	τ_z, τ_p
Implementation	Very easy	Complex	Easy	Average
Embedded Droop (Test 1)	Yes	No	No	No
Disturbance Rejection (Test 2)	Best	Bad	Bad	Average

VI. CONCLUSION

The smooth integration of RESs into the electric grid will require advanced control techniques for power electronics converters. To this purpose, a viable solution is the concept of VSM, which is capable of emulating and even outperforming traditional SMs. To obtain the best performance from VSMs, it is necessary to implement a correct electromechanical damping strategy. This way, the speed and power oscillations of the VSM are limited and the VSM-controlled inverter is enabled to damp low frequency oscillations in the power system. In this paper a damping solution for VSMs has been proposed and described. The proposed method consists of a single lead-lag filter on the active power feedback of VSMs, therefore representing a simple and straightforward solution with respect to most of the existing damping techniques available in the literature. Its performance was then validated experimentally and compared against three conventional damping methods for VSMs, leading to the summary comparison of Table I. The proposed lead-lag damping satisfies the requirement of full decoupling between the damping of the VSM and the frequency droop action of the plant, differently from the conventional droop-based damping. Moreover, the proposed method also features high rejection of any faulty condition in

the grid voltage, limiting the sensitivity of the VSM virtual speed against disturbances.

REFERENCES

[1] H. Bevrani, T. Ise, and Y. Miura, "Virtual synchronous generators: A survey and new perspectives," *International Journal of Electrical Power & Energy Systems*, vol. 54, pp. 244–254, Jan. 2014.

[2] M. Chen, D. Zhou, and F. Blaabjerg, "Modelling, Implementation, and Assessment of Virtual Synchronous Generator in Power Systems," *Journal of Modern Power Systems and Clean Energy*, vol. 8, no. 3, pp. 399–411, May 2020.

[3] U. Tamrakar, D. Shrestha, M. Maharjan, B. P. Bhattarai, T. M. Hansen, and R. Tonkoski, "Virtual Inertia: Current Trends and Future Directions," *Applied Sciences*, vol. 7, no. 7, p. 654, Jul. 2017.

[4] M. Ebrahimi, S. A. Khajehoddin, and M. Karimi-Ghartemani, "An Improved Damping Method for Virtual Synchronous Machines," *IEEE Transactions on Sustainable Energy*, vol. 10, no. 3, pp. 1491–1500, Jul. 2019.

[5] P. Kundur, *Power System Stability and Control*. McGraw-Hill Education, Jan. 1994.

[6] Q.-C. Zhong and G. Weiss, "Synchronverters: Inverters That Mimic Synchronous Generators," *IEEE Transactions on Industrial Electronics*, vol. 58, no. 4, pp. 1259–1267, Apr. 2011.

[7] S. D'Arco, J. A. Suul, and O. B. Fosso, "A Virtual Synchronous Machine implementation for distributed control of power converters in SmartGrids," *Electric Power Systems Research*, vol. 122, pp. 180–197, May 2015.

[8] M. Chen, D. Zhou, and F. Blaabjerg, "Active Power Oscillation Damping Based on Acceleration Control in Parallel Virtual Synchronous Generators System," *IEEE Transactions on Power Electronics*, pp. 1–1, 2021.

[9] H. Beck and R. Hesse, "Virtual synchronous machine," Oct. 2007, pp. 1–6.

[10] F. Mandrile, E. Carpaneto, and R. Bojoi, "Virtual Synchronous Generator with Simplified Single-Axis Damper Winding," in *2019 IEEE 28th International Symposium on Industrial Electronics (ISIE)*, Jun. 2019, pp. 2123–2128.

[11] L. Huang, H. Xin, H. Yuan, G. Wang, and P. Ju, "Damping Effect of Virtual Synchronous Machines Provided by a Dynamical Virtual Impedance," *IEEE Transactions on Energy Conversion*, pp. 1–1, 2020.

[12] F. Mandrile, E. Carpaneto, and R. Bojoi, "Grid-Feeding Inverter With Simplified Virtual Synchronous Compensator Providing Grid Services and Grid Support," *IEEE Transactions on Industry Applications*, vol. 57, no. 1, pp. 559–569, Jan. 2021.

[13] F. Mandrile, E. Carpaneto, E. Armando, and R. Bojoi, "Simple Tuning Method of Virtual Synchronous Generators Reactive Control," in *2020 IEEE Energy Conversion Congress and Exposition (ECCE)*, Oct. 2020, pp. 2779–2785.

[14] F. Mandrile, E. Carpaneto, and R. Bojoi, "VSG Simplified Damper Winding: Design Guidelines," in *IECON 2019 - 45th Annual Conference of the IEEE Industrial Electronics Society*, vol. 1, Oct. 2019, pp. 3962–3967.

[15] W. Zhang, D. Remon, and P. Rodriguez, "Frequency support characteristics of grid-interactive power converters based on the synchronous power controller," *IET Renewable Power Generation*, vol. 11, no. 4, pp. 470–479, 2017.

[16] X. Yan and S. Y. A. Mohamed, "Comparison of virtual synchronous generators dynamic responses," in *2018 IEEE 12th International Conference on Compatibility, Power Electronics and Power Engineering (CPE-POWERENG 2018)*, Apr. 2018, pp. 1–6.